

Excitation-Contraction Coupling in Airway Smooth Muscle*

Received for publication, July 10, 2006 Published, JBC Papers in Press, August 6, 2006, DOI 10.1074/jbc.M606541200

Wanglei Du[‡], Timothy J. McMahon[‡], Zhu-Shan Zhang[§], Jonathan A. Stiber[§], Gerhard Meissner[¶], and Jerry P. Eu^{‡1}

From the [‡]Division of Pulmonary, Allergy and Critical Care Medicine and [§]Division of Cardiology, Duke University, Medical Center, Durham, North Carolina, 27710 and the [¶]Department of Biochemistry and Biophysics, University of North Carolina, Chapel Hill, North Carolina 27599-7260

Excitation-contraction (EC) coupling in striated muscles is mediated by the cardiac or skeletal muscle isoform of voltage-dependent L-type Ca^{2+} channel ($\text{Ca}_v1.2$ and $\text{Ca}_v1.1$, respectively) that senses a depolarization of the cell membrane, and in response, activates its corresponding isoform of intracellular Ca^{2+} release channel/ryanodine receptor (RyR) to release stored Ca^{2+} , thereby initiating muscle contraction. Specifically, in cardiac muscle following cell membrane depolarization, $\text{Ca}_v1.2$ activates cardiac RyR (RyR2) through an influx of extracellular Ca^{2+} . In contrast, in skeletal muscle, $\text{Ca}_v1.1$ activates skeletal muscle RyR (RyR1) through a direct physical coupling that negates the need for extracellular Ca^{2+} . Since airway smooth muscle (ASM) expresses $\text{Ca}_v1.2$ and all three RyR isoforms, we examined whether a cardiac muscle type of EC coupling also mediates contraction in this tissue. We found that the sustained contractions of rat ASM preparations induced by depolarization with KCl were indeed partially reversed (~40%) by 200 μM ryanodine, thus indicating a functional coupling of L-type channels and RyRs in ASM. However, KCl still caused transient ASM contractions and stored Ca^{2+} release in cultured ASM cells without extracellular Ca^{2+} . Further analyses of rat ASM indicated that this tissue expresses as many as four L-type channel isoforms, including $\text{Ca}_v1.1$. Moreover, $\text{Ca}_v1.1$ and RyR1 in rat ASM cells have a similar distribution near the cell membrane in rat ASM cells and thus may be directly coupled as in skeletal muscle. Collectively, our data implicate that EC-coupling mechanisms in striated muscles may also broadly transduce diverse smooth muscle functions.

In cardiac muscle and in skeletal muscle, depolarization of the cell membrane causes voltage-dependent L-type Ca^{2+} channels localized to the cell membrane to activate the juxtaposing intracellular Ca^{2+} release channels known as ryanodine receptors (RyRs)² (1, 2). The massive release of Ca^{2+} from the

sarcoplasmic reticulum into the cytosol by activated RyRs then initiates a series of Ca^{2+} -dependent events that result in the cross-bridging of actin and myosin filaments, thereby completing the vital process of excitation-contraction (EC) coupling. The critical step of RyR activation by the L-type channels during EC coupling, however, differs between cardiac muscle and skeletal muscle. Specifically, in skeletal myocytes, the skeletal muscle isoform of L-type channel ($\text{Ca}_v1.1$) activates its corresponding isoform of RyR (RyR1) through direct physical coupling between the voltage-sensing, pore-forming α_1 subunit ($\text{Ca}_v1.1\alpha_1$ or α_{1S}) and the cytoplasmic domain of RyR1 (3, 4). In contrast, in cardiac myocytes, the cardiac RyR (RyR2) is activated by an influx of extracellular Ca^{2+} through the α_1 subunit of $\text{Ca}_v1.2$ ($\text{Ca}_v1.2\alpha_1$ or α_{1C}). Cardiac type of EC coupling therefore requires extracellular Ca^{2+} (i.e. Ca^{2+} -induced Ca^{2+} release), unlike the skeletal muscle type of EC coupling (2, 5).

An emerging body of literature now indicates that RyRs expressed in various smooth muscle types mediate many important pathophysiological processes. These processes include airway constriction (bronchoconstriction) (6, 7), the hallmark of asthma, and hypoxia-induced pulmonary vasoconstriction (8, 9), which enables ventilation-perfusion matching in the lung. However, unlike cardiac muscle or skeletal muscle that expresses one dominant RyR isoform, many smooth muscle types, including those in the airway, pulmonary and systemic vasculatures, and gastrointestinal tract, express all three RyR isoforms (7, 10–13). Existing data suggest that individual RyR isoforms in these smooth muscle tissues do not share the same activating mechanism (7, 10, 12, 14). However, how individual RyR isoforms are regulated in various smooth muscle tissues remains largely unknown.

Although recent studies have suggested that endogenous molecules such as cyclic ADP-ribose and FK506-binding proteins play a role in regulating stored Ca^{2+} release by RyRs in the airway smooth muscle (ASM) and in other smooth muscle types (14, 15), $\text{Ca}_v1.2$ and $\text{Ca}_v1.1$ remain the most firmly established physiological regulators of RyR2 and RyR1, respectively. Moreover, recent studies of ASM (7) and pulmonary arterial smooth muscle (11, 12) have shown that RyR1 and RyR2 appear to localize to portions of sarcoplasmic reticulum juxtaposing the cell membrane, thus raising the possibility that these RyR

* This work was supported by a departmental fund and by grants from the American Lung Association (North Carolina Chapter) and the American Heart Association (Mid-Atlantic Affiliate) (to J. P. E.) and National Institutes of Health Grant AR18687 (to G. M.). The costs of publication of this article were defrayed in part by the payment of page charges. This article must therefore be hereby marked "advertisement" in accordance with 18 U.S.C. Section 1734 solely to indicate this fact.

¹ To whom correspondence should be addressed: Division of Pulmonary, Allergy and Critical Care Medicine, MSRB 241, Research Dr., Duke University Medical Center, Durham, NC 27710. Tel.: 919-668-3832; Fax: 919-684-3067; E-mail: eu000001@duke.edu.

² The abbreviations used are: RyR, ryanodine receptor; RyR1, type 1 (skeletal muscle) RyR; RyR2, type 2 (cardiac) RyR; RyR3, type 3 (brain) RyR; EC, excitation-contraction; ASM, airway smooth muscle; $\text{Ca}_v1.2$, cardiac muscle isoform of L-type Ca^{2+} channel; $\text{Ca}_v1.1$, skeletal muscle isoform of L-type

Ca^{2+} channel; $\text{Ca}_v1.3$, neuro-endocrine isoform of L-type Ca^{2+} channel; $\text{Ca}_v1.1\alpha_1$ (α_{1S}), skeletal muscle isoform of α_1 subunit of L-type Ca^{2+} channel; $\text{Ca}_v1.2\alpha_1$ (α_{1C}), cardiac isoform of α_1 subunit of L-type Ca^{2+} channel; $\text{Ca}_v1.3\alpha_1$ (α_{1D}), neuro-endocrine isoform of α_1 subunit of L-type Ca^{2+} channel; $\text{Ca}_v1.4\alpha_1$ (α_{1F}), retinal isoform of α_1 subunit of L-type Ca^{2+} channel; KHB, Krebs-Henseleit buffer; RT, reverse transcription; PBS, phosphate-buffered saline.

Functional Coupling of L-Type Channels and RyRs in ASM

isoforms in certain smooth muscle types may also be functionally linked to the L-type channels in the cell membrane as in striated muscles. It is noteworthy that both L-type channels and RyRs in ASM and pulmonary arterial smooth muscles have been shown to mediate bronchoconstriction and hypoxia-induced pulmonary vasoconstriction (8, 9, 16–19), respectively. At present, it is not known whether L-type channels and RyRs mobilize Ca^{2+} independently or jointly to mediate these processes.

Since $\text{Ca}_v1.2$ is expressed in various smooth muscle types (20–22), we examined whether a cardiac muscle type of EC coupling in ASM may mediate contraction in this tissue. Here we report that the sustained, depolarization (KCl)-induced contractions of rat ASM preparations indeed were partially reversed by ryanodine, which specifically interacts with RyRs (1, 23), thus indicating the existence of EC coupling involving the L-type channels and RyRs in this tissue. However, in the absence of extracellular Ca^{2+} , KCl still caused transient contractions of these ASM preparations as well as Ca^{2+} release in cultured ASM cells. These data thus suggest the (co)existence of a skeletal muscle type EC-coupling mechanism in ASM. Our subsequent characterizations of the airway smooth muscle indicate that, in addition to $\text{Ca}_v1.2$, rat ASM expresses three other isoforms of L-type channels, as defined by their α_1 subunits. Moreover, $\text{Ca}_v1.1$ and RyR1 in rat ASM cells share a similar distribution near the cell membrane, thus suggesting a possible direct functional coupling between these two channels as in skeletal muscle. Collectively, our data indicate that ASM possesses every Ca^{2+} channel required for EC coupling in skeletal and cardiac muscles and thus suggest that EC-coupling mechanisms in striated muscles may also broadly transduce diverse smooth muscle functions.

EXPERIMENTAL PROCEDURES

Materials—The mouse monoclonal anti- $\text{Ca}_v1.1\alpha_1$ antibody and an anti-RyR antibody that recognizes RyR2 were obtained from Affinity BioReagents Inc (Golden, CO). Rabbit polyclonal anti- $\text{Ca}_v1.2\alpha_1$ and anti- $\text{Ca}_v1.3\alpha_1$ antibodies and their corresponding absorbing peptides were purchased from Calbiochem. The isoform specificities of anti- $\text{Ca}_v1.2\alpha_1$, anti- $\text{Ca}_v1.3\alpha_1$ were reported previously (7, 24). The isoform specificity of anti- $\text{Ca}_v1.1\alpha_1$ antibody is shown in Fig. 4A. A rabbit polyclonal anti-RyR1 antibody was raised against a synthetic peptide (CFIKGLDSFSGKPRGSG) and purified on peptide affinity column using a method similar to a method as described previously (25). The isoform specificity of the anti-RyR1 antibody was confirmed using rat heart homogenate and recombinantly expressed RyR3 protein as negative controls for RyR2 and RyR3, respectively (data not shown). Species-specific fluorescein-conjugated goat anti-mouse IgG and rhodamine-conjugated goat anti-rabbit IgG secondary antibodies were obtained from Jackson ImmunoResearch Laboratories (West Grove, PA). Ca^{2+} indicator Fura-2 acetoxymethyl ester was obtained from Molecular Probes (Eugene, OR). Cy3-conjugated mouse monoclonal anti-smooth muscle-specific α -actin IgG, ryanodine, and all other reagents were obtained from Sigma unless specified otherwise.

Depolarization-induced Contractile Responses of Rat ASM Preparations (Bronchial Rings)—Male Wistar rats (200–300 gm) were obtained from Charles River Laboratories. In a typical experiment, four second and third generation bronchial rings (inner diameter, ~ 1 mm, and length, ~ 3 mm) were isolated from each animal, dissected free of adventitial tissues, and studied in parallel as described previously (7). Briefly, each bronchial ring was mounted horizontally on two tungsten triangles and immersed in modified Krebs-Henseleit buffer (KHB, in mM, 118 NaCl, 4.8 KCl, 1.2 MgSO_4 , 1.2 KH_2PO_4 , 2.5 CaCl_2 , 25 NaHCO_3 , and 11 glucose, pH 7.4) warmed to 37 °C in a thermostated organ bath. The triangles (and thus the bronchial ring) were suspended between a stainless steel wire hook connected to a Grass FT-03 force displacement transducer (Grass-Telefactor, West Warwick, RI) and a glass hook inside the organ bath that served as an anchor. An optimal resting tension of 0.5 gm was applied to each ring during the initial equilibration period of 30 min, and the subsequent changes in isometric tension were amplified and recorded continuously (Polyview software, Grass-Telefactor). After the equilibration period, the bronchial rings were submaximally constricted with 40 mM KCl or maximally constricted with 80 mM KCl over 10 min to allow the contraction to reach steady state before adding 200 μM ryanodine to inhibit RyRs (1, 23).

In experiments to determine whether KCl could induce contractile responses in rat bronchial rings without extracellular Ca^{2+} , rat bronchial rings precontracted with 40 or 80 mM KCl for ~ 30 min were relaxed to the baseline by washing off high K^+ KHB with 3 volumes of modified KHB. After equilibration for another 10–20 min, the modified KHB was switched to Ca^{2+} -free KHB (in mM, 118 NaCl, 4.8 KCl, 1.2 MgSO_4 , 1.2 KH_2PO_4 , 25 NaHCO_3 , 11 glucose, and 0.5 EGTA, pH 7.4) for ~ 2 min before the rat bronchial rings were rechallenged with 80 or 40 mM KCl.

Depolarization-induced Ca^{2+} Responses of Rat ASM Cell in the Presence or Absence of Extracellular Ca^{2+} —ASM cells were isolated from the second and third generation of rat bronchi and cultured using a method described previously (7). After confirming that the majority ($>98\%$) of these cells expressed smooth muscle-specific α -actin, cells between two and four passages were grown in M199 media containing 10% fetal bovine serum over 7–8 days in culture dishes (MatTek, Ashland, MA) designed for live cell imaging. The ASM cells were first loaded with 5 μM Fura-2 acetoxymethyl ester in M199 media containing 10% fetal bovine serum for 30 min and then washed with modified KHB three times to remove excess Ca^{2+} indicator. In certain experiments, the ASM cells were washed twice more with Ca^{2+} -free KHB. The culture dish was then placed onto a stage mounted on an inverted microscope (Nikon Eclipse TE2000). The ASM cells were excited alternatively at 340 and 380 nm under ambient temperature (21 °C), and fluorescence measurements were performed on small groups of cells viewed with a Nikon UV-Fluor $\times 40$ oil-immersion objective as described previously (7). After an initial equilibration period of <2 min, 40 mM KCl was introduced, and the Ca^{2+} responses of ASM cells, in the presence or absence of extracellular Ca^{2+} , were reflected as changes in fluorescence ratio (F_{340}/F_{380}) of Fura-2 averaged from pixels within cytoplasmic

areas and recorded at 1-s intervals (7, 26). Each group of ASM cells were challenged with KCl only once.

Immunoblot Analyses of $Ca_v1\alpha_1$ and RyR Isoforms in Rat ASM—Second and third generation bronchi and trachea from rats were cleaned of adventitial tissues, pooled, and homogenized in a buffer consisting of 320 mM sucrose, 5 mM HEPES, and a protease inhibitor mixture (Complete Mini, Roche Applied Science) using a handheld tissue homogenizer. Membranous fractions enriched in Ca^{2+} channels were prepared from homogenates of rat ASM, skeletal muscle, heart, and brain tissues as described previously (7). The protein concentrations were determined using a Bio-Rad DC protein assay kit using albumin as a standard. Approximately 20–40 μ g of microsomal ASM protein samples were separated by 7% or 3–8% gradient Tris acetate SDS-PAGE under reducing conditions and transferred onto polyvinylidene fluoride membranes over 2 h. The membranes were first blocked with 5% nonfat milk in 0.05% Tween 20, phosphate-buffered saline (PBS) at 24 °C for 1 h. Following probing with anti- $Ca_v1.1\alpha_1$ (1 ng/ μ l), anti- $Ca_v1.2\alpha_1$ (1.5 ng/ μ l), anti- $Ca_v1.3\alpha_1$ (5 ng/ μ l), anti-RyR1 (1:100), and anti-RyR2 antibodies (7) overnight, the blots were developed using a Vectastain ABC-Amp Western blot detection kit (Vector Laboratories, Burlingame, CA) (7). To verify that protein bands observed in the immunoblots are indeed the isoforms of α_1 subunit of L-type channel, in certain experiments, the anti- $Ca_v1.2\alpha_1$ and anti- $Ca_v1.3\alpha_1$ antibody were preincubated with 1.5 ng/ μ l and 3.5 ng/ μ l corresponding absorbing peptide for 1 h before application (24).

RT-PCR Analyses of α_1 Subunit of L-type Channel ($Ca_v1\alpha_1$) and RyR Isoforms in Rat ASM—After removing adventitial and epithelial tissues, airway smooth muscle layers from trachea and large bronchi of each animal were pooled, and total RNA was extracted using the Qiagen RNeasy mini kit (Qiagen Inc., Carlsbad, CA) using a method described previously (7, 26). For real-time RT-PCR analysis of $Ca_v1\alpha_1$ isoforms, the first-strand cDNAs were synthesized from 200 ng of RNA from each sample using the Qiagen Sensiscript RT kit and resulted in a final sample volume of 40 μ l. After initial trials with different amounts of starting cDNAs, we amplified 2 μ l of cDNAs from each sample using the iQ SYBR Green Supermix and the iCycler iQ real-time PCR detection system (Bio-Rad Laboratories, Inc.). The isoform-specific forward and reverse primers are listed in Table 1. Rat β -actin was also amplified and used as an internal reference (10). The real-time PCR was run for one cycle at 95 °C for 3 min followed immediately by 40–45 cycles at 95 °C for 30 s, 56 °C for 30 s, and 72 °C for 60 s. The fluorescence was measured after each of the repetitive cycles. The PCR products for individual $Ca_v1\alpha_1$ isoforms amplified after 40 cycles were verified by electrophoresis and sequencing analyses (performed by Duke University DNA Sequencing Facility). Similarly, real-time RT-PCR analyses of RyR isoforms in rat ASM were performed using a protocol and isoform-specific primers described previously (7, 10).

Immunohistochemical Studies of $Ca_v1\alpha_1$ Isoforms in Rat Airways—Rat lung tissues were resected from euthanized animals, immediately immersed in Tissue-Tek[®] optimum cutting temperature compound (Sakura Finetek, Torrance, CA), and rapidly frozen in liquid nitrogen. Five- μ m sections were cut

onto glass slides and stored in –20 °C until the day of study. For immunohistochemical studies, the lung sections were dried in room temperature over 10 min, fixed with 2% paraformaldehyde in PBS (pH 7.4) for 10 min, and washed with PBS two more times. Subsequently, the tissue sections were quenched with 0.75% glycine and then permeabilized in 0.01% SDS and 0.1% Triton-X in PBS for 30 min. Before probing with individual antibody specific for each isoform of $Ca_v1\alpha_1$, the lung sections were treated using the M.O.M. kit (Vector Laboratories) according to the manufacturer's instructions to reduce background staining from endogenous immunoglobulins in the lung tissues. The dilutions for each of the antibodies were 1 ng/ μ l, 1.5 ng/ μ l, and 3.5 ng/ μ l for anti- $Ca_v1.1\alpha_1$, anti- $Ca_v1.2\alpha_1$, and anti- $Ca_v1.3\alpha_1$, respectively. After incubation with individual primary antibody for 1 h, the slides were stained using a VectaStain Elite kit (Vector Laboratories) according to the manufacturer's instructions. As with our immunoblot analyses, in certain experiments, the anti- $Ca_v1.2\alpha_1$ antibody and anti- $Ca_v1.3\alpha_1$ antibody were preincubated with the corresponding absorbing peptides before application (24). Each experiment also contained at least one control in which only the primary antibody was omitted. Small pieces of muscles from the hind leg, cardiac ventricle, and cardiac atria were used as positive control tissues for $Ca_v1.1\alpha_1$, $Ca_v1.2\alpha_1$, and $Ca_v1.3\alpha_1$, respectively (27). The slides were examined and digitally photographed using a microscope (Olympus BX60) equipped with UPlanFl $\times 10$ –20 objectives.

Immunofluorescence Study of RyR1 and $Ca_v1.1$ in Cultured Rat ASM Cells—To determine whether RyR1 and $Ca_v1.1$ are expressed in close proximity in rat ASM cells and therefore could be physically coupled as in skeletal muscle, immunofluorescence studies using the rabbit polyclonal anti-RyR1 (1:100 dilution) and the mouse monoclonal anti- $Ca_v1.1\alpha_1$ (1 ng/ μ l) were performed on non-overlapping, elongated rat ASM cells (~8 days old, third passage) using a method described previously (7). The ASM cells all expressed smooth muscle-specific α -actin, had KCl-induced Ca^{2+} responses (see Fig. 3), and had a similar RyR and $Ca_v1\alpha_1$ mRNA expression profile as intact rat ASM (see Fig. 7A). After double labeling with both primary antibodies, these cells were probed with species-specific fluorescein-conjugated goat anti-mouse IgG (7.5 ng/ μ l) and rhodamine-conjugated goat anti-rabbit IgG secondary antibodies (7.5 ng/ μ l) in 1% goat serum/PBS for 1 h before mounting on ProLong antifade solution (Molecular Probes). Control slides were prepared similarly except that primary antibodies were omitted. The prepared slides were then examined using a Carl Zeiss LSM 510 laser scanning confocal microscopy system attached to an Axiovert 100 inverted microscope equipped with a $\times 100$ objective as described previously (7).

Data Analysis—All results are expressed as means \pm S.E. Significance of differences of data were analyzed with Student's *t* test. A *p* value of < 0.05 was considered statistically significant.

RESULTS

Partial Reversal of KCl-induced Contractions of Rat ASM Preparations by Ryanodine—In rat bronchial rings maximally contracted with 80 mM KCl, the contractile responses were sus-

Functional Coupling of L-Type Channels and RyRs in ASM

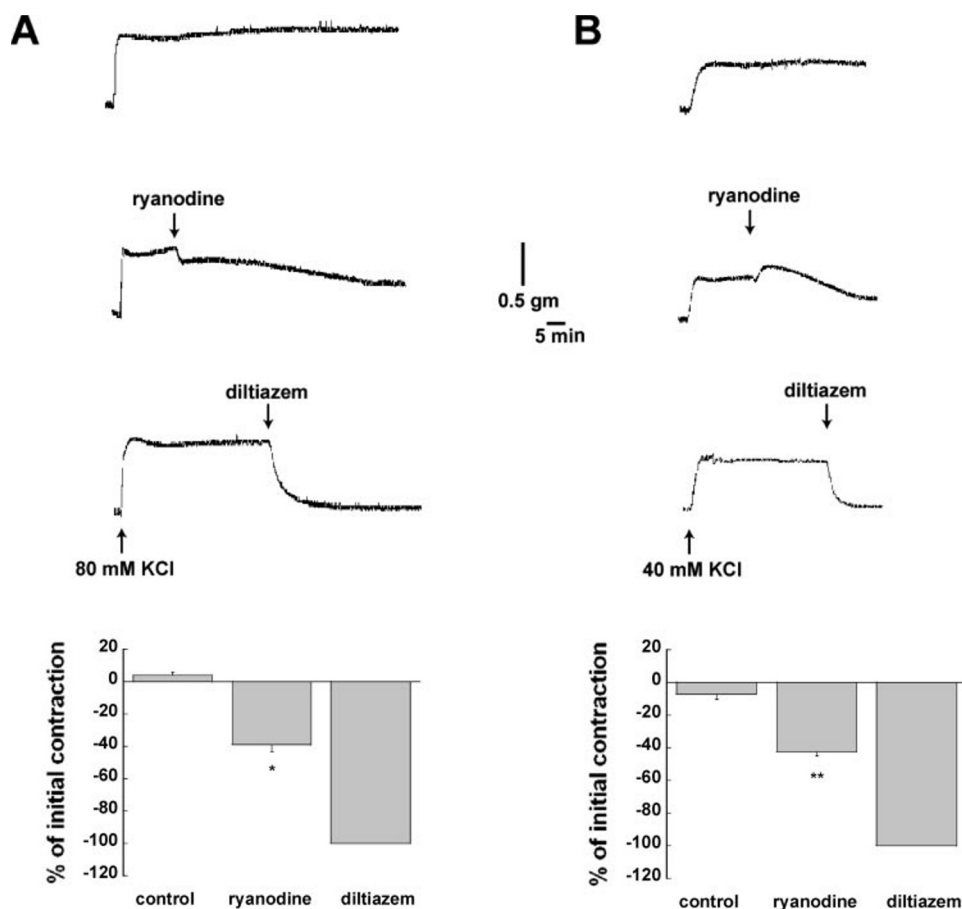


FIGURE 1. Partial reversal of depolarization-induced contractions of rat ASM preparations by inhibiting RyRs. Rat bronchial rings were maximally contracted by 80 mM KCl (A) or submaximally contracted by 40 mM KCl (B). As compared with time controls (*top traces*), adding 200 μ M ryanodine (*middle traces*) caused a gradual relaxation of rat bronchial rings. In the submaximally contracted bronchial rings, ryanodine caused a transient contraction before the gradual relaxation. Adding the L-type channel blocker 10 μ M diltiazem completely relaxed the KCl-contracted bronchial rings (*lower traces*). Combined data of maximally (A, *bottom panel*) and submaximally (B, *bottom panel*) contracted bronchial rings in response to ryanodine or diltiazem at steady state (mean \pm S.E., $n = 5$ in each group). *, $p < 0.005$, and **, $p < 0.001$ versus corresponding time control groups.

tained for more than 1 h (Fig. 1A, *top trace*). In contrast, inhibition of RyRs by adding 200 μ M ryanodine (1, 23) caused a partial relaxation that continued over 30 min before stabilization (Fig. 1A, *middle trace*). The KCl-induced contractions of bronchial rings are mediated by voltage-dependent L-type channels (28) as the L-type channel blocker diltiazem (10 μ M) completely reversed the contraction (Fig. 1A, *bottom trace*). In bronchial rings submaximally contracted by 40 mM KCl (Fig. 1B), 200 μ M ryanodine caused an additional transient contraction before the partial relaxation. This biphasic response of submaximally contracted bronchial rings to ryanodine is likely due to some remaining stored Ca^{2+} release by RyRs in ASM as ryanodine entering the ASM activates RyRs at lower concentrations (1). The biphasic responses of rat bronchial rings to ryanodine were observed in every submaximally contracted ring but never in maximally contracted bronchial rings ($n = 5$ in each group). At steady state (~ 1 h after applying KCl), ryanodine significantly reversed the initial KCl-induced contraction in both 80 mM and 40 mM KCl-contracted rat bronchial rings by 38.8 ± 4.5 and $42.3 \pm 2.7\%$, respectively (Fig. 1C, $p < 0.001$ versus the corresponding control groups). These data thus indicate a func-

tional coupling of L-type channels and RyRs in the depolarization/KCl-induced contractions of rat ASM preparations.

Depolarization-induced Transient Contractions of Rat ASM Preparations in the Absence of Extracellular Ca^{2+} —Since the effect of 200 μ M ryanodine on KCl-contracted bronchial rings indicates the existence of EC coupling in ASM and $Ca_v1.2$ is thought to be the main L-type isoform in smooth muscle tissues (20–22), we examined whether extracellular Ca^{2+} is essential for KCl-induced contractions of rat ASM preparations. This requirement for extracellular Ca^{2+} would support the notion that EC coupling in the ASM is entirely mediated by an influx of Ca^{2+} (via L-type channels) that subsequently activates RyRs analogous to the cardiac muscle type of EC coupling (*i.e.* Ca^{2+} -induced Ca^{2+} release) (2). Unexpectedly, every rat bronchial ring contracted in response to 40 or 80 mM KCl in the absence of extracellular Ca^{2+} (and in the presence of 0.5 mM EGTA, $n = 8$ in each group). However, the contractile responses of these bronchial rings without extracellular Ca^{2+} were transient and smaller than the corresponding contractile responses in the presence of extracellular Ca^{2+} (Fig. 2B). The peak KCl-induced contractile

responses of bronchial rings in the absence of extracellular Ca^{2+} were $79.9 \pm 3.2\%$ of the corresponding responses in the presence of extracellular Ca^{2+} in the 80 mM KCl group and $41 \pm 5.2\%$ in the 40 mM KCl group (Fig. 2B). Moreover, most of the KCl-induced contractions in the absence of extracellular Ca^{2+} ended within 5 min, suggesting that extracellular Ca^{2+} is needed to replenish intracellular Ca^{2+} stores. Nevertheless, these data suggest that depolarization of ASM cell membrane causes stored Ca^{2+} release in rat ASM without extracellular Ca^{2+} , thus suggesting the (co)existence of a skeletal muscle type of EC coupling in ASM.

Depolarization-induced Stored Ca^{2+} Release in Cultured Rat ASM Cells in the Absence of Extracellular Ca^{2+} —To confirm that KCl-induced contractions of ASM preparations in the absence of extracellular Ca^{2+} are due to stored Ca^{2+} release, we directly monitored intracellular Ca^{2+} concentrations ($[Ca^{2+}]_i$) of cultured ASM cells isolated from second and third generations of rat bronchi. The majority (>98%) of these ASM cells expressed smooth muscle cell-specific α -actin. We subsequently found that these cultured ASM cells expressed a similar profile of Ca^{2+} channel mRNAs as ASM tissue even after five

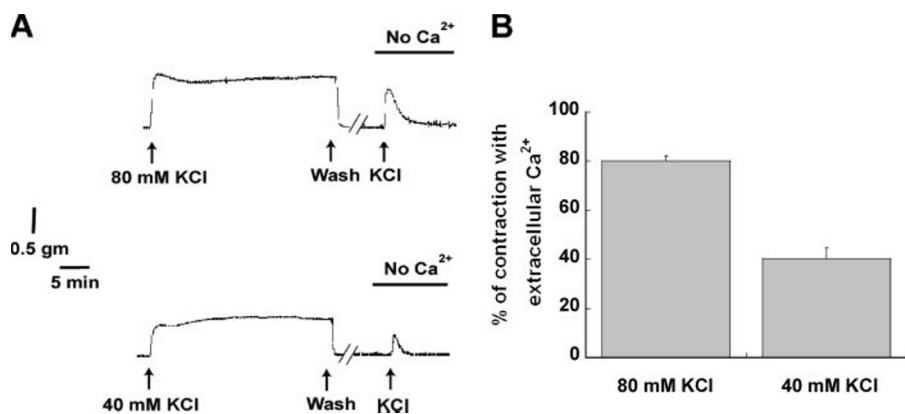


FIGURE 2. **Contractile responses of rat ASM preparations to KCl in the absence of extracellular Ca^{2+} .** Rat bronchial rings were maximally or submaximally contracted with 80 mM (A, top panel) or 40 mM KCl (A, lower panel), respectively, for ~ 30 min before switching to modified KHB containing 0.5 mM EGTA and without Ca^{2+} as indicated by the top bars. Rat bronchial rings were then rechallenged with KCl (arrows). B, relative peak contractile responses of rat bronchial rings to 80 or 40 mM KCl in the absence of extracellular Ca^{2+} (mean \pm S.E.).

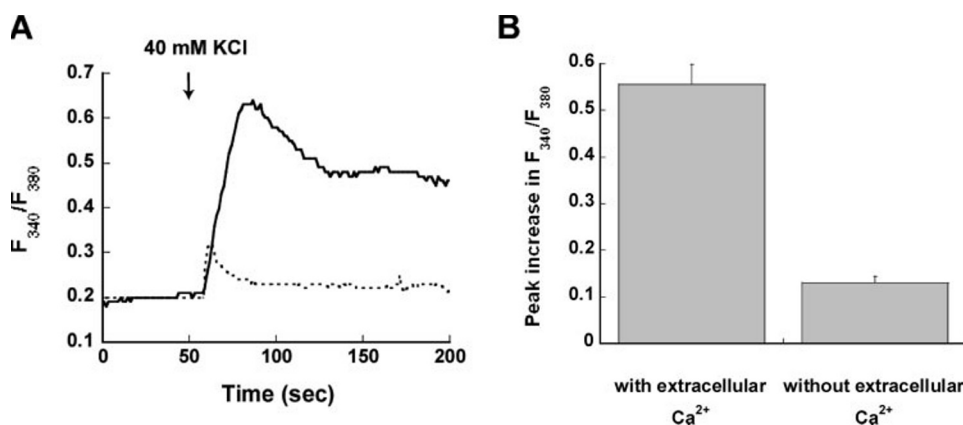


FIGURE 3. **Ca^{2+} responses of cultured rat ASM cells to KCl in the absence of extracellular Ca^{2+} .** A, in cultured rat ASM cells all expressing smooth muscle-specific α -actin, representative Ca^{2+} responses of cultured rat ASM cells to 40 mM KCl in the presence (solid trace) or absence (dotted trace) of extracellular Ca^{2+} . KCl was added at ~ 60 s (arrow). B, combined peak Ca^{2+} responses of cultured ASM cells to 40 mM KCl with or without extracellular Ca^{2+} .

passages (see Figs. 5B and 7A). The changes in $[\text{Ca}^{2+}]_i$ of these cells were reflected by changes in the fluorescence ratio of Fura-2 (F_{340}/F_{380}) averaged from pixels within cytoplasmic areas. In the presence of extracellular Ca^{2+} , 40 mM KCl typically induced a large initial Ca^{2+} transient but then maintained a stable Ca^{2+} above the resting state ($n = 49$, Fig. 3A, solid trace). In ASM cells depolarized with 40 mM KCl in the absence of extracellular Ca^{2+} ($n = 25$), the peak increases in $[\text{Ca}^{2+}]_i$ were significantly lower than those in cells in the presence of extracellular Ca^{2+} (Fig. 3, A and B).

Expression of Multiple L-type Channel and RyR Isoforms in the Rat Airways—The *ex vivo* studies of rat ASM preparations and cultured ASM cells both suggest that EC coupling in ASM is not completely dependent on extracellular Ca^{2+} , thus indicating the (co)existence of skeletal muscle type EC coupling in this tissue. Since all three RyR isoforms are expressed in mouse ASM (7), we used immunoblot techniques to examine the membranous fractions of rat ASM homogenate for L-type channel isoforms that may transduce the skeletal muscle type of EC coupling in this tissue. Commercially available antibodies that recognize individual isoforms of voltage-sensing, pore-

forming α_1 subunit ($\text{Ca}_v1\alpha_1$), which defines the L-type channel isoform, were used. Rat skeletal muscle, heart, and brain were used as positive control tissues for $\text{Ca}_v1.1\alpha_1$, $\text{Ca}_v1.2\alpha_1$, and $\text{Ca}_v1.3\alpha_1$, respectively (24, 29). $\text{Ca}_v1.4\alpha_1$ was not included in our immunoblot studies due to the lack of availability of an isoform-specific antibody. In positive control tissues (Fig. 4, A–C), each $\text{Ca}_v1\alpha_1$ isoform appeared as double bands with molecular masses of ~ 200 kDa in immunoblots, indicating the expression of both a full-length channel and a truncated channel, as has been described previously (24, 29). Rat ASM also expressed both full-length and truncated $\text{Ca}_v1.2\alpha_1$ channels (Fig. 4B, left panel). In immunoblots probed with anti- $\text{Ca}_v1.2\alpha_1$ preincubated with $\text{Ca}_v1.2\alpha_1$ -absorbing peptides (24), the double bands seen in both rat ASM and heart samples were eliminated (Fig. 4B, right panel).

However, rat ASM also expresses both $\text{Ca}_v1.1\alpha_1$ and $\text{Ca}_v1.3\alpha_1$ proteins with molecular masses slightly above 195 kDa. In ASM, $\text{Ca}_v1.1\alpha_1$ exists as a truncated protein, but a faint protein that corresponds to the full-length channel was also seen in two out of five experiments (Fig. 4A, left panel). In certain experiments, membranous fractions from rat brain and heart were used as con-

trols to test this anti- $\text{Ca}_v1.1\alpha_1$ antibody isoform specificity (Fig. 4A, right panel). In contrast to $\text{Ca}_v1.1\alpha_1$ and $\text{Ca}_v1.2\alpha_1$, $\text{Ca}_v1.3\alpha_1$ in ASM exists only as a full-length channel ($n =$ three independent experiments, Fig. 4C, left panel). In immunoblot experiments in which the anti- $\text{Ca}_v1.3\alpha_1$ was preincubated with $\text{Ca}_v1.3\alpha_1$ -absorbing peptides, the protein band in the ASM sample along with two protein bands in the brain samples were eliminated (Fig. 4C, right panel) and then surfaced after reprob-ing these blots with anti- $\text{Ca}_v1.3\alpha_1$ alone (data not shown). Another protein band with a molecular mass slightly below 200 kDa in the brain sample was not affected by the $\text{Ca}_v1.3\alpha_1$ -absorbing peptides (Fig. 4C, arrow). The identity of this protein band is not known. As reported in mouse ASM (7) and rat pulmonary arterial smooth muscle (11, 12), rat ASM also expresses multiple isoforms of RyRs. In particular, our immunoblot studies of membranous fractions from rat ASM using anti-RyR antibodies suggested the presence of both RyR1 and RyR2 (Fig. 4D).

To confirm the existence of multiple L-type channel isoforms in ASM, including $\text{Ca}_v1.1\alpha_1$ that may transduce the depolarization-induced contractions of ASM in the absence of extracellular Ca^{2+} (Fig. 2), we performed RT-PCR analyses on

Functional Coupling of L-Type Channels and RyRs in ASM

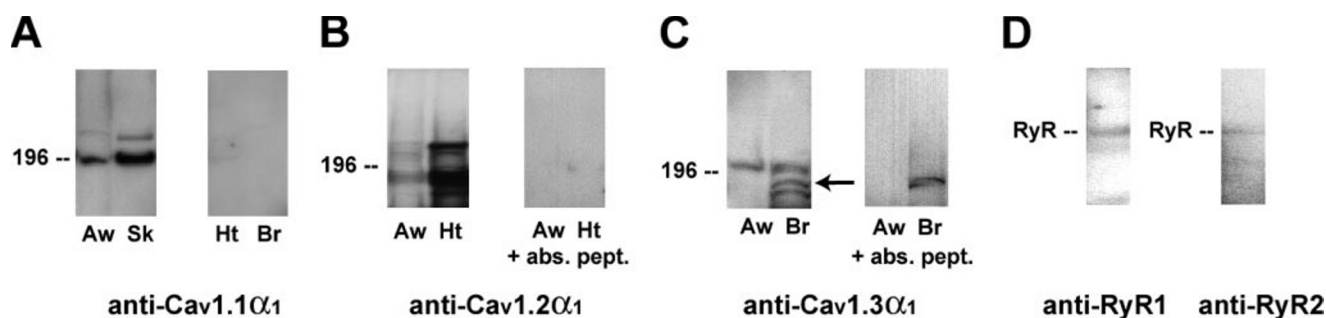


FIGURE 4. Expression of L-type channel and RyR proteins in rat ASM. Membranous fractions of rat ASM (*Aw*), heart (*Ht*), skeletal muscle (*Sk*), or brain (*Br*) were probed with the individual isoform-specific anti- $\text{Ca}_v1\alpha_1$ antibody labeled below (*A*, *B*, and *C*, left panels). In certain experiments, blots were probed with anti- $\text{Ca}_v1.2\alpha_1$ antibody or anti- $\text{Ca}_v1.3\alpha_1$ antibody preincubated with corresponding absorbing peptides (*abs. pept.*) as labeled (*B* and *C*, right panel). In *C*, the arrow indicates the protein band that was not eliminated by anti- $\text{Ca}_v1.3\alpha_1$ -absorbing peptide. Each blot is representative of at least three independent experiments. RyR1 and RyR2 are expressed in rat ASM as described previously in rat pulmonary arterial smooth muscle (11, 12) and mouse ASM (7) (*D*).

TABLE 1
Primers for rat isoforms of α_1 subunit of L-type Ca^{2+} channels

Gene	Accession number	Primer	Sequence 5'-3'	Nucleotide position	Predicted size
$\text{Ca}_v1.1\alpha_1$	RATCACAI	Sense	TGTGGTATGTCGTCACCTTCCTCC	1193-1215	258
		Antisense	CGTCAATGATGCTGCCAATG	1450-1431	
$\text{Ca}_v1.2\alpha_1$	NM012517.1	Sense	CAAGCCCTCGCAGAGGAATGC	5198-5218	232
		Antisense	GAAGTTGCTCCTGCTGTCACCTC	5429-5408	
$\text{Ca}_v1.3\alpha_1$	NM017298.1	Sense	CCATCTCACACCCGCGGACTATG	6842-6865	500
		Antisense	CATCACCTTGACCTCTCTCGTG	7341-7319	
$\text{Ca}_v1.4\alpha_1$	NM053701.1	Sense	GATTTGCCCATCCAGGCACCTAC	5487-5510	445
		Antisense	CATCAAAGCGGGAGAGAATAGACTC	5931-5907	

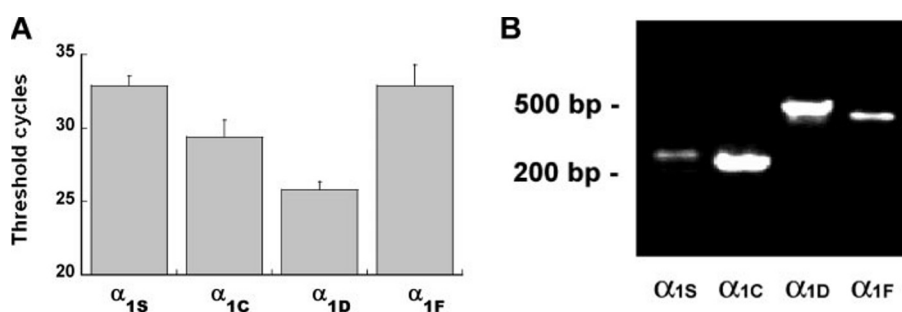


FIGURE 5. Expression of L-type channel mRNAs in rat ASM. *A*, real-time RT-PCR analyses using isoform-specific primers for each $\text{Ca}_v1\alpha_1$ isoform labeled at the bottom ($\text{Ca}_v1.1\alpha_1 = \alpha_{1S}$; $\text{Ca}_v1.2\alpha_1 = \alpha_{1C}$; $\text{Ca}_v1.3\alpha_1 = \alpha_{1D}$; and $\text{Ca}_v1.4\alpha_1 = \alpha_{1F}$) ($n =$ three independent experiments in each group). The PCR products amplified over 40 cycles were subjected to electrophoresis and had the expected molecular weights (*B*).

rat ASM. Real-time RT-PCR analyses of rat ASM using primers specific for each rat α_1 subunit (Table 1) revealed mRNAs for all four known $\text{Ca}_v1\alpha_1$ isoforms. The individual RT-PCR products were verified by electrophoresis and had the expected molecular weights of 258 ($\text{Ca}_v1.1\alpha_1$), 232 ($\text{Ca}_v1.2\alpha_1$), 500 ($\text{Ca}_v1.3\alpha_1$), and 445 ($\text{Ca}_v1.4\alpha_1$) bp (Fig. 5*B*). The identity of each $\text{Ca}_v1\alpha_1$ product was further confirmed by sequencing analyses (Table 2). The RT-PCR products of $\text{Ca}_v1.2\alpha_1$ and $\text{Ca}_v1.3\alpha_1$, as judged by their lower detection threshold cycles in the real-time RT-PCR and in electrophoresis analyses, appear to be more abundant than those of $\text{Ca}_v1.1\alpha_1$ and $\text{Ca}_v1.4\alpha_1$ (Fig. 5).

As with mouse ASM (7), RyR1 and RyR2 were detected in rat ASM (Fig. 4*D*). Collectively, our data indicate that rat ASM expresses all of the Ca^{2+} channels (*i.e.* RyR1, RyR2, $\text{Ca}_v1.1\alpha_1$, and $\text{Ca}_v1.2\alpha_1$) essential for EC coupling in cardiac and skeletal muscles.

Expression of Multiple $\text{Ca}_v1\alpha_1$ Isoforms in the Rat ASM—To confirm that each $\text{Ca}_v1\alpha_1$ isoform detected by immunoblot

and RT-PCR analyses is expressed within the ASM layer of bronchi (and was not due to contamination by other cell types in the airways), we performed immunohistochemical studies on frozen-sectioned rat lung tissues using individual isoform-specific anti- $\text{Ca}_v1\alpha_1$ antibodies as in our immunoblot studies. The three α_1 isoforms were all detected within the smooth muscle layers (as highlighted by a Cy-3-conjugated anti-smooth muscle-specific α -actin antibody) of large rat bronchi (Fig. 6, *second upper panel* from the left).

In addition, anti- $\text{Ca}_v1.2\alpha_1$ antibody may also recognize an antigen in the epithelial layer of airway. In frozen lung sections probed only with the goat anti-mouse IgG secondary antibody or with the goat anti-rabbit IgG secondary antibody, only background staining was detected in the airway (Fig. 6, *left lower panels*). Moreover, in control experiments in which the anti- $\text{Ca}_v1.2\alpha_1$ or anti- $\text{Ca}_v1.3\alpha_1$ antibody was preincubated with its corresponding absorbing peptides, the immunohistochemical staining of the smooth muscle layers was significantly reduced (Fig. 6, *right lower panels*).

RyR1 and $\text{Ca}_v1.1\alpha_1$ Are Expressed in Close Proximity in Rat ASM Cells—We and others previously used a mouse anti-RyR1 IgM antibody to show that RyR1 is expressed near the cell membrane of ASM cells (7) and pulmonary arterial smooth muscle cells (11, 12). To determine whether RyR1 and $\text{Ca}_v1.1\alpha_1$ are expressed in close proximity in rat ASM cells (and therefore could be functionally coupled), we performed a co-localization

TABLE 2

Partial sequences of the RT-PCR products and the matched rat genes

Product no.	Sequence	Matched accession no.	Nucleotide position	Gene
1	5'-GGAACAGATGAACCACATATCGGACATCC TCAATGTGGCTTTCACCATCATCTTCACCCT-3'	RATCACAI	1290-1349	Ca _v 1.1α ₁
2	5'-AGGAGGAGCTGGACAAGGCTATGAAGGAG GCAGTGTCTGCCTCCGAAGACGACATCT-3'	NM012517.1	5302-5361	Ca _v 1.2α ₁
3	5'-TGGCAGATGAAATGATTGCATCACCACCT TGTAGCCCGAGGAGAGCAGGCTTGGCTCCA-3'	NM017298.1	6932-6991	Ca _v 1.3α ₁
4	5'-CCTGTGCTGGTGGAGGAATCTACAGTGGG TGAAGGATACCTTGGCAAGCTCGGCGGCC-3'	NM053701.1	5594-5653	Ca _v 1.4α ₁

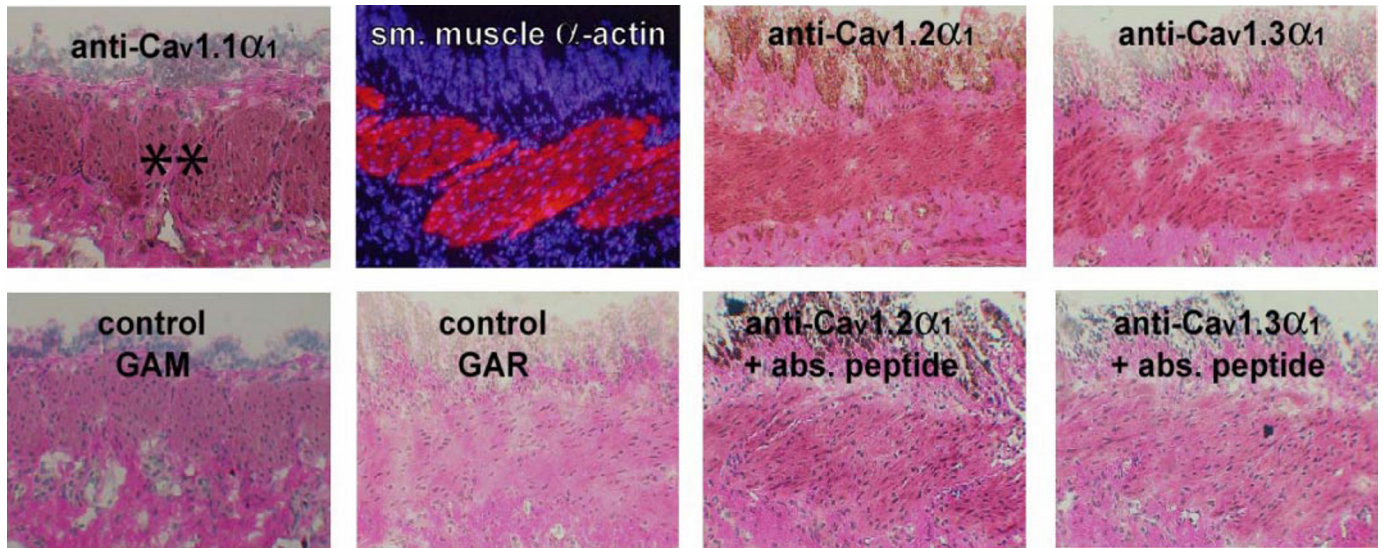


FIGURE 6. Immunohistochemical detection of L-type channel isoform in rat ASM. Rat lung tissues containing large bronchi were probed with individual isoform-specific anti-Ca_v1α₁ antibodies (*top panels*). The individual antigens were detected by 3, 3'-diaminobenzidine staining in ASM (labeled **) and also highlighted by the immunofluorescence staining for smooth muscle (*sm. muscle*)-specific α-actin. In addition, control experiments were performed in which only the secondary antibody goat anti-mouse IgG (*GAM*) or goat anti-rabbit IgG (*GAR*) was used (*left lower panels*). In other control experiments, anti-Ca_v1.2α₁ and anti-Ca_v1.3α₁ were preincubated with their corresponding absorbing peptides (*abs. peptide*) as labeled before their application (*right lower panels*). Each picture is representative of three independent experiments.

study of these two Ca²⁺ channels using immunofluorescence techniques. In this study, rabbit anti-RyR1 IgG was used instead of mouse anti-RyR1 IgM as our control experiments indicated that the fluorochrome-labeled secondary antibodies could not reliably distinguish between the mouse IgM (anti-RyR1) and mouse IgG (anti-Ca_v1.1α₁) antibodies. These cultured ASM cells expressed a similar profile of Ca²⁺ channel mRNAs as the rat ASM (Fig. 7A). As shown in Fig. 7B, RyR1 and Ca_v1.1α₁ share similar cellular distribution in cultured rat ASM cells. Near the cell membrane (Fig. 7B, *arrows*), there were areas of overlaps between RyR1 and Ca_v1.1α₁, thus suggesting co-localization and a possible physical coupling of these two channels in ASM cells.

DISCUSSION

Although Ca_v1.2 is thought to be the main L-type channel isoform in smooth muscle tissues (20), herein we describe that ASM also expresses other isoforms of L-type Ca²⁺ channels, including the skeletal muscle isoform Ca_v1.1 (Figs. 4–6). Since ASM also expresses RyR1 and RyR2 (Figs. 4 and 6) (7), ASM thus possesses all of the Ca²⁺ channels involved in the EC coupling of striated muscles (30). Moreover, the reversal of depolarization-induced rat ASM contractions by RyR inhibition (200 μM ryanodine (1, 23)), as shown in Fig. 1, indicates that the depolarizing signals in the cell membrane of ASM are also

transmitted to the sarcoplasmic reticulum via L-type channels, thereby leading to stored Ca²⁺ release by RyRs (*i.e.* EC coupling in ASM). As our immunofluorescence studies of ASM cells indicate that RyR1 and Ca_v1.1 are expressed in close proximity (Fig. 7) and ASM preparations contracted in response to depolarization in the absence of extracellular Ca²⁺ (Fig. 2) (28), our data collectively suggest the (co)existence of the skeletal muscle type of EC coupling in ASM.

Since a previous study has also demonstrated that both RyR1 and RyR2 are essential in the KCl-induced Ca²⁺ responses of rat portal venous smooth muscle cells (10), EC-coupling mechanisms in striated muscles may exist in other smooth muscle tissues. As mentioned previously, both L-type channels and RyRs in various types of smooth muscle have been implicated in mediating important pathophysiological processes that include bronchoconstriction and hypoxia-induced pulmonary vasoconstriction (8, 9, 16–19). Thus, EC coupling of RyR and L-type channel may be broadly involved in diverse smooth muscle functions.

Although the results described herein are from studies using rat ASM, similar reversal of KCl-induced contractions of ASM preparations by RyR inhibition (Fig. 1) and expression of multiple isoforms of L-type channel α₁ subunit at mRNA level were also observed in studies of mouse ASM preparations (data not shown). We chose to focus on rat ASM in this study because

Functional Coupling of L-Type Channels and RyRs in ASM

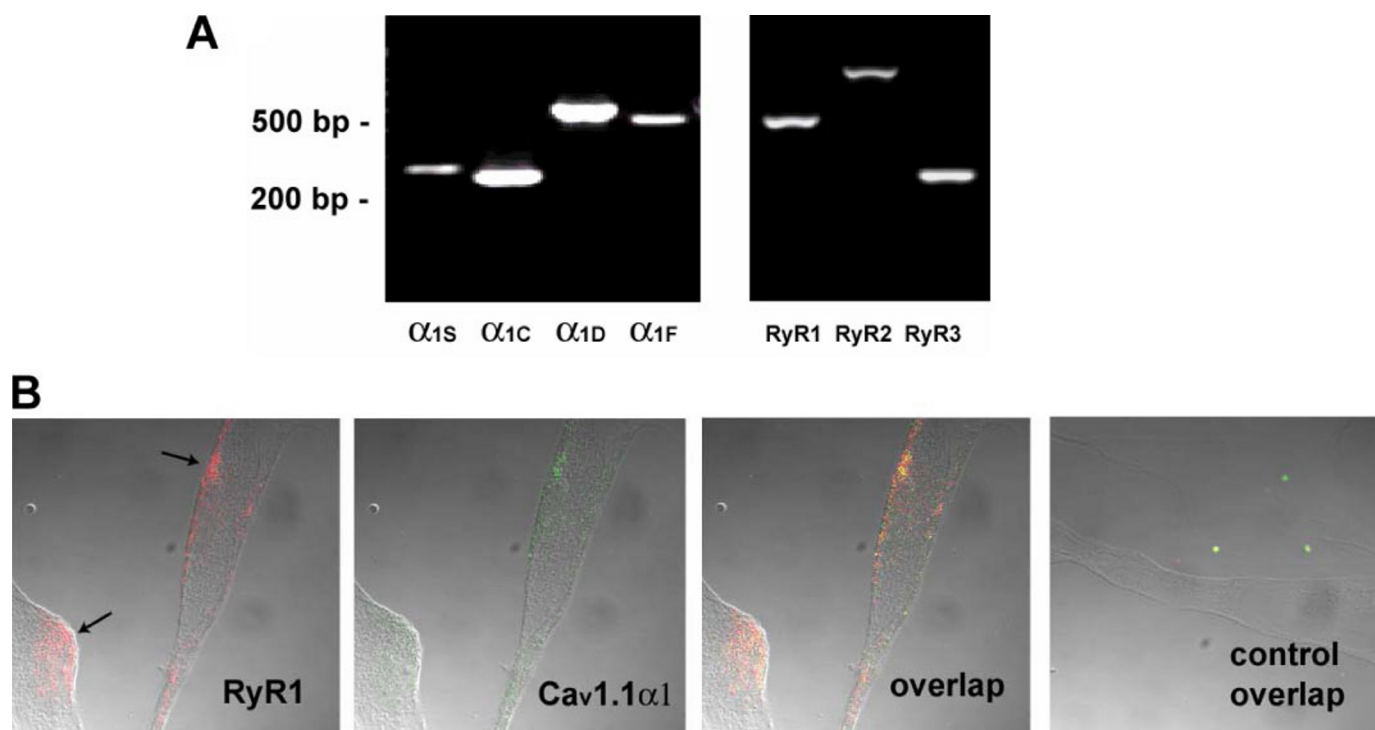


FIGURE 7. Co-localization of RyR1 and $Ca_v1.3\alpha_1$ in cultured rat ASM cells. Cultured rat ASM cells expressed a profile of Ca^{2+} channel mRNAs similar to that of ASM shown in Fig. 4 (A). $Ca_v1.1\alpha_1 = \alpha_{1S}$; $Ca_v1.2\alpha_1 = \alpha_{1C}$; $Ca_v1.3\alpha_1 = \alpha_{1D}$; and $Ca_v1.4\alpha_1 = \alpha_{1F}$. In these cells, RyR1 (pseudo-red fluorescence) and $Ca_v1.1\alpha_1$ (pseudo-green fluorescence) appear to have a similar distribution and are overlapped in areas near the cell membrane (B, arrows). Control cells were probed with both secondary antibodies but without the primary antibodies.

immunohistochemical studies of mouse lung tissues using mouse primary antibodies were confounded by a high background staining from the endogenous mouse immunoglobulins in these tissues. The larger ASM preparations from rat, as expected, produced larger and therefore less ambiguous KCl-induced contractile responses. Moreover, the larger amount of ASM tissues obtained from rats facilitated our immunoblot studies.

Because ASM plays a central role in many respiratory disorders such as asthma and chronic obstructive pulmonary disease, it has been studied extensively. Moreover, L-type Ca^{2+} channels in ASM play a central role in the Ca^{2+} responses of ASM, including those provoked by prototypic airway spasmogens, the muscarinic receptor agonists (17, 19). Yet our study is the first detailed analysis of L-type channel isoforms in ASM. Similarly, characterizations of L-type channel isoforms have not been performed on most smooth muscle types despite the critical roles of the Ca^{2+} channels in regulating vascular tone, gas exchanges, gastrointestinal peristalsis, and other vital functions. In this study, we used a combination of techniques to demonstrate that rat ASM expresses multiple isoforms of L-type channels, as defined by their voltage-sensing, pore-forming α_1 subunits. It remains unknown as to the roles of these L-type channel isoforms in ASM. We speculate that the multiple Ca_v1 isoforms in ASM, possibly pairing with the corresponding isoform of RyRs, may play a role in the graded contractile responses of ASM to incremental doses of airway spasmogens as these different Ca_v1 isoforms have different thresholds and/or mechanisms of activation (31).

Although it is difficult to make firm conclusions regarding

the relative expression of various L-type channel isoforms, we noted that the expression of $Ca_v1.3\alpha_1$ in the ASM is robust (Figs. 4 and 5). Whether $Ca_v1.3\alpha_1$ in ASM may be functionally coupled to RyRs is not known and thus will require further studies. Although the functional role of $Ca_v1.3\alpha_1$ in ASM remains unknown, the existence of $Ca_v1.3\alpha_1$ in ASM helps explain previous findings that L-type channels in the ASM can be activated at a relatively more negative potential (32). $Ca_v1.3\alpha_1$ has been shown to be activated at membrane potentials ~ 15 – 25 mV more hyperpolarized than $Ca_v1.2\alpha_1$ (33, 34). Unlike knocking out $Ca_v1.1$ or $Ca_v1.2$, knocking out $Ca_v1.3$ is not lethal (27). Thus, studying mice deficient in $Ca_v1.3$ could be helpful in further assessing the functions of this L-type channel isoform in ASM and in other smooth muscle types.

Our findings suggesting that $Ca_v1.1$ and RyR1 are functionally coupled in ASM also have other implications. In skeletal muscle, the physical coupling of these two Ca^{2+} channels not only allows EC coupling; reciprocal activation of $Ca_v1.1$ by RyR1 also facilitates Ca^{2+} entry into skeletal muscle to replenish intracellular Ca^{2+} stores (35, 36). This type of reciprocal activation of L-type channels by RyRs has also been described in neurons (37). Since it has been reported previously that muscarinic agonist-induced contraction of ASM requires replenishment of intracellular Ca^{2+} stores by L-type channels (38–40), a functional coupling of RyR1 and $Ca_v1.1$ may subserve to replenish Ca^{2+} stores in ASM in muscarinic agonist-induced bronchoconstriction.

In summary, we have found that ASM expresses multiple isoforms of L-type channels, and at least one of these isoforms is functionally coupled to the RyRs in ASM. As we already

described that ASM expresses all three RyR isoforms, we conclude that this tissue contains all of the Ca²⁺ channels required for EC coupling in skeletal and cardiac muscles. Since both L-type channels and RyRs play vital roles in such important pathophysiological processes such as bronchoconstriction and hypoxia-induced pulmonary vasoconstriction, collectively, our data suggest that the mechanisms of EC coupling in skeletal muscle and cardiac muscle may also be exploited by various smooth muscle types to effect their diverse functions.

Acknowledgment—We thank Dr. Augustus O. Grant for technical assistance and suggestions.

REFERENCES

1. Franzini-Armstrong, C., and Protasi, F. (1997) *Physiol. Rev.* **77**, 699–729
2. Meissner, G. (1994) *Annu. Rev. Physiol.* **56**, 485–508
3. Tanabe, T., Beam, K. G., Adams, B. A., Niidome, T., and Numa, S. (1990) *Nature* **346**, 567–569
4. Tanabe, T., Beam, K. G., Powell, J. A., and Numa, S. (1988) *Nature* **336**, 134–139
5. Fill, M., and Copello, J. A. (2002) *Physiol. Rev.* **82**, 893–922
6. Bergner, A., and Sanderson, M. J. (2002) *J. Gen. Physiol.* **119**, 187–198
7. Du, W., Stiber, J. A., Rosenberg, P. B., Meissner, G., and Eu, J. P. (2005) *J. Biol. Chem.* **280**, 26287–26294
8. Gelband, C. H., and Gelband, H. (1997) *Circulation* **96**, 3647–3654
9. Jabr, R. I., Toland, H., Gelband, C. H., Wang, X. X., and Hume, J. R. (1997) *Br. J. Pharmacol.* **122**, 21–30
10. Coussin, F., Macrez, N., Morel, J. L., and Mironneau, J. (2000) *J. Biol. Chem.* **275**, 9596–9603
11. Yang, X. R., Lin, M. J., Yip, K. P., Jeyakumar, L. H., Fleischer, S., Leung, G. P., and Sham, J. S. (2005) *Am. J. Physiol.* **289**, L338–L348
12. Zheng, Y. M., Wang, Q. S., Rathore, R., Zhang, W. H., Mazurkiewicz, J. E., Sorrentino, V., Singer, H. A., Kotlikoff, M. I., and Wang, Y. X. (2005) *J. Gen. Physiol.* **125**, 427–440
13. Fritz, N., Macrez, N., Mironneau, J., Jeyakumar, L. H., Fleischer, S., and Morel, J. L. (2005) *J. Cell Sci.* **118**, 2261–2270
14. Wang, Y. X., Zheng, Y. M., Mei, Q. B., Wang, Q. S., Collier, M. L., Fleischer, S., Xin, H. B., and Kotlikoff, M. I. (2004) *Am. J. Physiol.* **286**, C538–C546
15. Deshpande, D. A., White, T. A., Dogan, S., Walseth, T. F., Panettieri, R. A., and Kannan, M. S. (2005) *Am. J. Physiol.* **288**, L773–L788
16. Weir, E. K., Lopez-Barneo, J., Buckler, K. J., and Archer, S. L. (2005) *N. Engl. J. Med.* **353**, 2042–2055
17. Fanta, C. H., Venugopalan, C. S., Lacouture, P. G., and Drazen, J. M. (1982) *Am. Rev. Respir. Dis.* **125**, 61–66
18. Morio, Y., and McMurtry, I. F. (2002) *J. Appl. Physiol.* **92**, 527–534
19. Tomasic, M., Boyle, J. P., Worley, J. F., III, and Kotlikoff, M. I. (1992) *Am. J. Physiol.* **263**, C106–C113
20. Catterall, W. A., Perez-Reyes, E., Snutch, T. P., and Striessnig, J. (2005) *Pharmacol. Rev.* **57**, 411–425
21. Kovac, J. R., Preiksaitis, H. G., and Sims, S. M. (2005) *Am. J. Physiol.* **289**, G998–G1006
22. Moosmang, S., Schulla, V., Welling, A., Feil, R., Feil, S., Wegener, J. W., Hofmann, F., and Klugbauer, N. (2003) *EMBO J.* **22**, 6027–6034
23. Sutko, J. L., and Airey, J. A. (1996) *Physiol. Rev.* **76**, 1027–1071
24. Hell, J. W., Westenbroek, R. E., Warner, C., Ahljanian, M. K., Prystay, W., Gilbert, M. M., Snutch, T. P., and Catterall, W. A. (1993) *J. Cell Biol.* **123**, 949–962
25. Protasi, F., Takekura, H., Wang, Y., Chen, S. R., Meissner, G., Allen, P. D., and Franzini-Armstrong, C. (2000) *Biophys. J.* **79**, 2494–2508
26. Rosenberg, P., Hawkins, A., Stiber, J., Shelton, J. M., Hutcheson, K., Bassel-Duby, R., Shin, D. M., Yan, Z., and Williams, R. S. (2004) *Proc. Natl. Acad. Sci. U. S. A.* **101**, 9387–9392
27. Zhang, Z., He, Y., Tuteja, D., Xu, D., Timofeyev, V., Zhang, Q., Glatzer, K. A., Xu, Y., Shin, H. S., Low, R., and Chiamvimonvat, N. (2005) *Circulation* **112**, 1936–1944
28. Janssen, L. J., Tazzeo, T., Zuo, J., Pertens, E., and Keshavjee, S. (2004) *Am. J. Physiol.* **287**, L852–L858
29. Morton, M. E., and Froehner, S. C. (1987) *J. Biol. Chem.* **262**, 11904–11907
30. Meissner, G. (2004) *Cell Calcium* **35**, 621–628
31. Catterall, W. A. (2000) *Annu. Rev. Cell Dev. Biol.* **16**, 521–555
32. Fleischmann, B. K., Murray, R. K., and Kotlikoff, M. I. (1994) *Proc. Natl. Acad. Sci. U. S. A.* **91**, 11914–11918
33. Xu, W., and Lipscombe, D. (2001) *J. Neurosci.* **21**, 5944–5951
34. Koschak, A., Reimer, D., Huber, I., Grabner, M., Glossmann, H., Engel, J., and Striessnig, J. (2001) *J. Biol. Chem.* **276**, 22100–22106
35. Nakai, J., Dirksen, R. T., Nguyen, H. T., Pessah, I. N., Beam, K. G., and Allen, P. D. (1996) *Nature* **380**, 72–75
36. Nakai, J., Sekiguchi, N., Rando, T. A., Allen, P. D., and Beam, K. G. (1998) *J. Biol. Chem.* **273**, 13403–13406
37. Chavis, P., Fagni, L., Lansman, J. B., and Bockaert, J. (1996) *Nature* **382**, 719–722
38. Bourreau, J. P., Abela, A. P., Kwan, C. Y., and Daniel, E. E. (1991) *Am. J. Physiol.* **261**, C497–C505
39. Bourreau, J. P., Kwan, C. Y., and Daniel, E. E. (1993) *Am. J. Physiol.* **265**, C28–C35
40. Janssen, L. J. (2002) *Am. J. Physiol.* **282**, L1161–L1178